

Article

Investigation of Algal Biotoxin Removal during SWRO Desalination through a Materials Flow Analysis

Derek C. Manheim and Sunny C. Jiang * 

Department of Civil and Environmental Engineering, University of California, Irvine, CA 92697, USA; dmanheim@uci.edu

* Correspondence: sjiang@uci.edu; Tel.: +1949-824-5527

Received: 19 August 2017; Accepted: 19 September 2017; Published: 23 September 2017

Abstract: The operation of seawater reverse osmosis (SWRO) desalination facilities has become challenged by the increasing frequency and severity of harmful algal blooms (HABs). The efficiency of algal toxins removal during SWRO and pretreatment processes has critical human health implications. Therefore, a probabilistic materials flow analysis (pMFA) was developed to predict the removal of algal toxins in source water by various pretreatment configurations and operations during SWRO desalination. The results demonstrated that an appreciable quantity of toxins exists in the SWRO permeate (ng/L– μ g/L levels), the backwash of pretreatment, and final brine rejects (μ g/L–mg/L levels). Varying the pretreatment train configuration resulted in statistically significant differences in toxin removals, where higher removal efficiencies were evidenced in systems employing microfiltration/ultrafiltration (MF/UF) over granular media filtration (GMF). However, this performance depended on operational practices including coagulant addition and transmembrane pressures of MF/UF systems. Acute human health risks during lifetime exposure to algal toxins from ingestion of desalinated water were benign, with margins of safety ranging from 100 to 4000. This study highlights the importance of pretreatment steps during SWRO operation in the removal of algal toxins for managing marine HABs.

Keywords: harmful algal blooms; marine algal toxins; SWRO pretreatment; human health risks

1. Introduction

Seawater reverse osmosis (SWRO) technology has the potential to meet the growing worldwide demand for freshwater by securing the most abundant resource of surface water available on the planet: the ocean [1]. As the stress increases on existing surface freshwater supplies due to population growth, agricultural development, global climate change, and industrial expansion, SWRO has become a more accepted approach to augment the world's existing freshwater supply, especially in arid regions such as the Middle East [2,3]. Coupled with recent advances in membrane technology and sustainable sources of energy for operation (such as solar or wind power), SWRO is transitioning from a viable alternative to an integral component of freshwater provisions for many coastal municipalities and industries worldwide [4–7].

Like any emerging technology, however, SWRO faces several important challenges to gain full acceptance as a reliable technology for freshwater supply [7]. The increasing frequency and severity of harmful marine algal blooms (HABs), has posed a serious threat to full-scale SWRO desalination facilities operating worldwide [8–10]. Caron and co-workers [11] acknowledged two important impacts of HABs on desalination facilities: (1) complete removal of algal toxins; (2) increased demand on pretreatment for membrane fouling prevention. Besides the elevated biomass, algal blooms also

contribute to excess organic matter and transparent exopolymer particles (TEP) that intensify the biofouling potential of SWRO membranes [12–14].

Although HABs cannot be prevented entirely, engineering measures have been developed to overcome the issues encountered. Existing responses to HABs at SWRO facilities may include changes to the operation or design of pretreatment trains. Operational changes may include increasing coagulant/flocculant addition, reducing filtration (granular or membrane based) run times, and increasing backwashing intensity or cleaning frequency of filtration systems [1,12]. More recently, amendments to the design of pretreatment trains may include integrating dissolved air flotation (DAF) systems or changing inline coagulation/flocculation systems to an individual unit treatment process with separate sedimentation tanks to improve algal cell removal [14].

Increased awareness of the harmful effects of HABs on full-scale desalination processes has also prompted new monitoring techniques and associated numerical modeling efforts to predict HAB events, so plant engineers and operators can be better prepared to handle the negative effects of these bloom periods on plant operations [11,14]. Integrating online sensing systems—such as fluorescent light scattering (i.e., flow cytometry) and/or total organic carbon analyzers—with RO membranes also provides a direct way to both detect and assess the deleterious effects of HAB periods on permeate water quality [15].

A topic often overlooked, however, is the fate of marine algal biotoxins throughout pretreatment and RO membrane operations in full-scale desalination facilities [9,16]. Most existing studies in the literature have been limited to examining removal of these marine algal toxins across RO membranes alone, concluding that the RO membranes remove a considerable portion (>99%) of dissolved algal toxins [8–10,16]. However, these studies were restricted to the laboratory/pilot scale of analysis and did not consider the effects of pretreatment processes on toxin removal.

In addition, the associated human health risk from consumption of desalinated water during HABs has not been fully assessed [8–10,16]. Preliminary risk assessments have ascertained that the risk of acute intoxication from consumption of desalinated water is rather low [8–10]. However, these assessments were based on data acquired from laboratory-based studies, and may severely underestimate the environmental and hydraulic conditions RO membranes face in practice. The environmental effects of the backwash water and brine rejects during HAB periods are even less understood and are under-reported in the scientific literature [11]. Therefore, a probabilistic materials flow analysis (pMFA) was carried out in this study to gain a quantitative and holistic understanding of the removal of algal biotoxins during full-scale SWRO practice. Ultimately, the pMFA was developed to answer the following questions: What is the typical concentration of algal toxins in desalinated water and brine/reject water? What pretreatment designs and operations (if any) lead to improved algal toxin removals? What is the human health risk from drinking desalinated water during HABs?

To address these questions, a quantitative comparison of toxin removal efficiencies during pre-treatment for several conventional configurations was conducted to estimate the toxin concentration in the RO permeate as well as the combined pretreatment backwash and brine reject. A formal risk assessment framework was adopted to estimate the acute human health risks from drinking desalinated water incorporating the posterior distributions of toxin concentrations from the pMFA output. Model parameter sensitivity and outcome confidence evaluations were conducted to ascertain the validity of the model predictions and to prioritize future data collection efforts.

2. Materials and Methods

2.1. pMFA Overview and Model Assumptions

A pMFA was used to simulate the fate of algal toxins through various treatment processes [17,18]. To best represent a realistic desalination system, the study was set in Coastal Southern California, a region actively exploring SWRO as a solution to supplement ever increasing drinking water demands, where at least six new facilities have been proposed [19]. A hypothetical 50 million gallons per day

(MGD) ($1.89 \times 10^5 \text{ m}^3/\text{day}$) SWRO desalination facility, located in Santa Monica Bay, CA, was used to set the theoretical control volume for the pMFA analysis. The system would operate with a conventional salt rejection rate of 99.5%, permeate recovery of 50%, and intake rate of 100 MGD ($3.78 \times 10^5 \text{ m}^3/\text{day}$). A period of 24 h was set as the duration of the pMFA for facility operation, providing a daily perspective on marine algal toxin production and fate in a SWRO facility.

The conceptual pMFA diagram that includes 10 distinct pretreatment trains commonly used in a conventional full-scale desalination facility is shown in Figure 1 (T1—T10). At the intake, the marine algal toxins enter in either dissolved (extracellular, C_{E0} in $\mu\text{g}/\text{L}$) or particulate (intracellular, C_{I0} in pg/cell) forms. The mass flow of intracellular (M_{I0}) and extracellular toxins (M_{E0}) entering the facility is calculated using Equations (1) and (2).

$$M_{I0} = C_A * V_I * C_{I0} \tag{1}$$

$$M_{E0} = C_{E0} * V_I \tag{2}$$

where C_A is the count of algal cells in intake water (cells/L), V_I is the intake volume, C_{I0} and C_{E0} is the intracellular toxin per cell (pg/cell) and extracellular toxin per liter ($\mu\text{g}/\text{L}$), respectively.

Following the intake into the desalination facility, conventional coagulation treatment is considered for each process train with no sedimentation; consequently, no mass of toxin is removed during this step. Treatment trains without the coagulation step were also used for comparison (Figure 1). In addition, comparisons were made for trains with and without DAF before treatment options of: pressurized microfiltration/ultrafiltration (MF/UF), submerged MF/UF (vacuum), gravity granular media filtration (GMF), and pressurized GMF. The volumetric inflow and backwash for each pretreatment process in the pMFA are detailed in the Supplementary Materials, Section 1.

For each pretreatment process a range of toxin removal efficiencies (transfer coefficients) were specified. These parameters included: (a) removal of intracellular toxins within intact cells during pretreatment processes (K_1); (b) removal of dissolved toxins during pretreatment processes (K_2); and (c) removal of dissolved toxins across the RO membrane (K_3). An additional model parameter was specified to account for the release of intracellular toxin to dissolved toxin as a result of algal cell breakage during each pretreatment process (K_B).

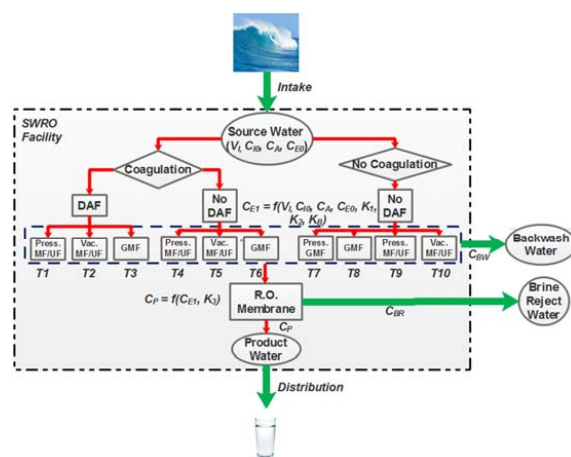


Figure 1. Conceptual pMFA diagram for the full-scale SWRO desalination facility. The boundaries of the SWRO facility are indicated by the dashed black line, while pretreatment unit processes trains (T1—T10) are grouped by the dashed blue line. The arrows indicate toxin mass flow rates expressed in $\mu\text{g}/\text{day}$, simplifying to a mass of toxin (in μg) on the timescale of one day. The red arrows specify mass flows within the desalination facility control volume, whereas the green arrows indicate mass flows of toxins out of the control volume.

The core calculations of the pMFA for the combined pretreatment and RO membrane processes included three main steps. First, the mass of intracellular toxin in intact algal cells (M_{NB} , μg) and that released (M_B , μg) due to the cell breakage fraction, K_B , were determined (Equations (3) and (4)).

$$M_{NB} = (M_{I0} - K_B * M_{I0}) \quad (3)$$

$$M_B = (1 - M_{NB}) \quad (4)$$

Next, the dissolved toxin concentration (C_{E1} , $\mu\text{g/L}$) and backwash toxin concentration (C_{BW} , $\mu\text{g/L}$) after treatment by a given unit treatment process were calculated using the dissolved toxin (K_1) and cellular toxin (K_2) removal coefficients and the volume of intake water (V_I , L) and backwash water (V_{BW}) (Equations (5) and (6)).

$$C_{E1} = \frac{(M_{E0} - (K_1 * M_{E0}) + M_B) + (M_{NB} - K_2 * (M_{NB}))}{V_I} \quad (5)$$

$$C_{BW} = \frac{(K_1 * M_{E0}) + (K_2 * M_{NB})}{V_{BW}} \quad (6)$$

Finally, the concentration of dissolved toxin in the RO permeate water (C_p , $\mu\text{g/L}$) and RO brine water rejects (C_{BR} , $\mu\text{g/L}$) were calculated considering the removal efficiency across the RO membrane (K_3), the volume of permeate water (V_p , L) and brine/reject water (V_{BR} , L) (Equations (7) and (8)). The mass of extracellular toxin entering final RO treatment (M_{E1} , μg) was calculated assuming that all intact cells remaining (M_{NB} , μg) were ruptured due to the high-pressure RO membrane process.

$$C_p = \frac{(M_{E1} - K_3 * M_{E1})}{V_p} \quad (7)$$

$$C_{BR} = \frac{(K_3 * M_{E1})}{V_{BR}} \quad (8)$$

Several assumptions were included to reduce the model complexity: (1) no biological removal mechanisms were involved due to the lack of published information and the complexity of predicting removal; (2) toxins were dissolved into solution upon cell breakage; and (3) no generation or storage mechanisms for any treatment train processes were considered—flow that entered each treatment process had to leave either in the backwash/concentrate waters or water flowing through the RO membrane.

2.2. Algal and Toxins Concentrations

Algal bloom data at the Santa Monica Pier were taken from the Southern California Coastal Ocean Observing System (SCCOOS, <http://www.sccoos.org/>), which reports common bloom formers including *Akashiwo sanguinea*, *Alexandrium* species, *Dinophysis* species, *Prorocentrum* species, *Lingulodinium polyedrum*, *Pseudo-nitzschia* species, *Cochlodinium* species, and *Phaeocystis* species. It is important to note that the *Pseudo-nitzschia* cell abundance data included in the SCCOOS database is not currently identified down to the species level [20]. Instead, cell abundance is classified into two different size fractions by light microscopy: the *Pseudo-nitzschia delicatissima* class (frustule widths $>3 \mu\text{m}$) and the *Pseudo-nitzschia seriata* class (frustule widths $<3 \mu\text{m}$) [20]. Of these genera listed, only some species of *Alexandrium* (producer of saxitoxin, STX), *Dinophysis* (producer of okadaic acid, OA), *Lingulodinium polyedrum* (producer of yessotoxin, YTX), and *Pseudo-nitzschia* (producer of domoic acid, DA) produce toxins [11]. Therefore, only DA, STX, OA, and YTX were included in the pMFA. The toxic effects of each toxin are described in the Supplementary Materials, Section 2.

SCCOOS data from a three-year period (2012–2015) were first used to create an overview of the frequency and severity of blooms in the region, similar to the time-period specified by Seubert and co-workers [20] (Figure S1). To simplify the pMFA analysis, we did not separate bloom

periods into either major or minor events as previously described [20–22]. Instead, a constant chlorophyll-a threshold using the overall mean of the 3-year data (~12 µg/L) was incorporated to identify significant events (comparable to the definition for minor blooms in [21]). From this analysis, eight significant bloom events were identified (chlorophyll-a >12 µg/L). DA producing species exhibited the highest cell abundance and variation over each of the eight bloom periods (Table 1), confirming blooms off Southern California were greatly dominated by *Pseudo-nitzschia* sp. [11,23]. STX (*Alexandrium*) and YTX (*L. polyedrum*) producing species were the least abundant and variable in cell numbers during the bloom periods (Table 1 and Figure S2).

The statistical distributions of cell concentrations from the bloom periods appeared to be nonparametric (after excluding 0 and non-detects), with higher frequency of observations at the lower range in cell concentrations (see Supplementary Materials Figure S3). Therefore, to adequately predict cell concentrations in pMFA simulations, an inverse empirical concentration distribution function (ECDF) was developed relating the probability of occurrence (x-axis) versus the concentration (\log_{10}) of species observed from field data (see Supplementary Materials Figure S4). To account for the probability of non-detects, a uniform random number generator between 0 and 1 was first used. The selection was then sent to sample the corresponding cell concentration from the interpolated, inverse ECDF.

In comparison with algal cell concentrations, data on dissolved toxin concentrations surrounding Santa Monica Pier was sparse. Limited dissolved toxin concentrations (DA, STX) reported at the intake of a Southern and Central California SWRO pilot facilities [10,16] indicated lower (0–10 µg/L) ranges than those observed in coastal and inland marine or estuarine environments (0–150 µg/L) [21–23]. These data were perhaps not collected during a substantial algal bloom. Thus, coastal and inland marine measurements [24–26] collected off the west coast of the continental U.S. were considered more representative of severe HAB scenarios and were used in this analysis (Table 1). However, dissolved toxin concentrations for OA and YTX were compiled from work by Mackenzie and co-workers [27], which were collected off the coast of New Zealand (Table 1).

Table 1. Concentration of dissolved marine toxins, toxin producing algal cells and intracellular toxin per cell used in the pMFA simulations.

Environmental Variable	Distribution	Unit	Specified Range or Value	Mean	SD	Reference
<i>Dissolved toxins</i>						
DA	Uniform	µg/L	60–135.6	-	-	[24,25]
STX	Uniform	µg/L	0.150–0.800	-	-	[26]
OA	Uniform	µg/L	1.31–4.67	-	-	[27]
YTX	Uniform	µg/L	23.7–126	-	-	[27]
<i>Algal cell conc.</i> ¹						
<i>Alexandrium</i> sp.	ECDF	cells/L	374–748	524	205	
<i>Dinophysis</i> sp.	ECDF	cells/L	123–3886	1112	1120	
<i>L. polyedrum</i>	ECDF	cells/L	374–748	481	183	
<i>Pseudo-nitzschia delicatissima</i>	ECDF	cells/L	374–48,578	15,170	35,896	
<i>Pseudo-nitzschia seriata</i>	ECDF	cells/L	374–563,500	22,280	92,575	
<i>Intracellular toxin conc.</i>						
<i>Alexandrium</i> sp.	Uniform	pg/cell	57.9	-	-	[28]
<i>Dinophysis</i> sp.	Uniform	pg/cell	2.7	-	-	[29]
<i>L. polyedrum</i> ²	Uniform	pg/cell	0.005	-	-	[30]
<i>Pseudo-nitzschia delicatissima</i>	Uniform	pg/cell	117	-	-	[23]
<i>Pseudo-nitzschia seriata</i>	Uniform	pg/cell	117	-	-	[23]

¹ All algal cell concentrations were retrieved from SCCOOS Database; ² This value was collected from laboratory-grown cells.

Only dissolved concentrations obtained by grab sampling as opposed to passive sampling methods (SPATT) were included in this analysis given that it is not currently possible to directly

compare or extrapolate SPATT measurements ($\mu\text{g/g}$ resin) to ambient concentrations ($\mu\text{g/L}$). SPATT integrates sampling both spatially and temporally and, in many cases, has been evidenced to be more sensitive than grab sampling methods [31,32]. Although adsorption profiles and extraction efficiencies of these toxins (DA, STX) to/from SPATT resins have been extensively studied and verified in the laboratory setting, this knowledge is not applicable to uncontrolled conditions in the field setting, leading to instances of moderate variability in replicate field measurements (coefficients of variation (COV) 15–37%) [32]. This observed variability in SPATT measurements further supports reliance on grab measurements reported from field studies, where COV for replicate measurements are $<10\%$ for ELISA kits (per manufacturer instructions, ABRAXIS, Warminster, PA, USA). Uniform probability distributions were used in the modeling effort due to the lack of published information reporting dissolved toxin concentrations (Table 1).

The intracellular toxin concentrations reported from most field and laboratory studies were highly variable in the scientific literature [23,28,29]. Intracellular toxin concentrations of DA as determined from laboratory cultures of *Pseudo-nitzschia* species, for example, were observed to vary over 9 orders of magnitude [33]. Field reported values of intracellular toxin concentrations were less common and were also highly variable due to different physical, chemical, and biological factors influencing bloom dynamics in field settings (see [34] for additional information). Due to the lack of understanding of the intracellular concentration of most species (which likely varies with environmental conditions, the phase of the algal bloom, etc.), the highest reported intracellular concentration from field reports was used as the model input to represent a worst-case scenario (Table 1). A deterministic value of intracellular toxin concentration was further used to continue with the conservative, worst-case scenario approach. In the absence of field studies, YTX intracellular toxin concentrations were obtained from a laboratory study of *L. polyedrum* isolated from coastal Southern California waters [30].

2.3. Intracellular and Dissolved Toxin Removal Efficiencies

The removal efficiency of intracellular toxin was directly related to the removal of toxin producing algal cells during each pretreatment process. Algal cell removals through GMF systems were compiled based on pilot or full-scale SWRO studies reported in the literature (Table 2) [16,35–42]. A pooled mean and standard deviation of algal cell removal for GMF systems with and without coagulation was calculated and fitted to a normal probability distribution (Table 2). However, a uniform probability distribution was used for predicting cell removal in pressurized GMF systems due to the lack of data in the published literature (Table 2).

For MF/UF systems, the range in algal cell removal efficiencies was also summarized from pilot and full-scale SWRO plant studies [38,43–46]. Uniform probability distributions were used in the pMFA model for MF/UF systems considering the small number of reported observations from the literature (Table 2).

Table 2. Intracellular and dissolved toxin removal efficiencies used in the pMFA simulations.

Treatment Trains	Specified Range	Reference
<i>Cell Removal</i>		
GMF With Coagulation	79–93% ¹	[36,38,40]
GMF Without Coagulation	48–98% ¹	[37,39,41]
GMF Pressurized	74–99.2%	[16,35,42]
MF/UF With Coagulation	99–99.9%	[16,42]
MF/UF Without Coagulation	95–100%	[38,43–46]
DAF	43–93%	[42,47,48]
RO	-	-

Table 2. Cont.

Treatment Trains	Specified Range	Reference
<i>Algal Cell Breakage</i> ²		
GMF With Coagulation	0–10%	This study
GMF Without Coagulation	0–25%	This study
GMF Pressurized	75–100%	This study
MF/UF With Coagulation	75–100% (pressure driven); 15–35% (submerged)	This study
MF/UF Without Coagulation	50–100% (pressure driven); 15–35% (submerged)	This study
DAF	-	-
RO	-	-
<i>Dissolved toxin removal</i> ³		
GMF With Coagulation	0–34%	This study
GMF Without Coagulation	26–50%	This study
GMF Pressurized	6.6–40%	This study
MF/UF With Coagulation	24.7–76.7%	This study
MF/UF Without Coagulation	3–32.7%	This study
DAF	-	-
RO	99.4–99.9%	[8,10,16]

¹ The mean and standard deviation are 86% and 11%, respectively for cell removal by GMF with coagulation; and are 72% and 21%, respectively for cell removal by GMF without coagulation. The mean and deviation were not calculated for the remaining parameters in the table due to limited data availability; ² Estimated based on transmembrane pressure used in each pretreatment process (see Supplementary Materials, Section 3.6 for details); ³ Estimated based on toxin physical-chemical properties and reference toxin removal rates (see Supplementary Materials, Sections 3.1–3.4 for details).

DAF algal cell removals were obtained from reports of a mixture of laboratory, pilot, and full-scale experiments [42,47,48]. The reported range in algal cell removal efficiencies ranged between 43–93%, likely due to the variations in algal cells encountered and doses/types of coagulants used (Table 2). Again, uniform probability distributions were used in the pMFA model for predicting algal cell removals in DAF systems.

An important consideration during pretreatment for cell removal is algal cell breakage that transforms intracellular toxins into dissolved toxins. The magnitude of the ranges in algal cell breakage was developed according to Voutchkov [12] (see Supplementary Materials, Section 3.6) and differed for each pretreatment process (Table 2). The wide ranges in cell breakage used here reflect the expected variability in breakage among different species and groups (diatoms versus dinoflagellates) of marine microalgae. However, the increments of the ranges (set to quartiles, i.e., 25–50%, 75–100%) were relatively similar for different treatment processes as a conservative factor in all pMFA simulations. Since DAF processes use air bubbles to float the algal cells to the surface, no algal cell breakage was expected. In addition, due to the small molecular size, water solubility, and polarity of the toxins, little to no removal of dissolved toxins was expected in the DAF process.

An extensive literature search indicated a lack of data on the dissolved marine algal toxin removal rates through SWRO pretreatment trains. However, removal efficiencies of dissolved microcystin-LR (MC-LR) toxins produced by cyanobacteria that impact drinking water safety have been reported in both GMF and MF/UF processes. Therefore, the removal efficiencies of each targeted marine algal toxin were estimated based on a comparison of the physical-chemical properties (including size, structure, polarity and charge) of each with those of MC-LR (Table 2) (see Supplementary Materials, Section 3 and Tables S6–S8 for additional validation). Uniform probability distributions sampled the range of dissolved toxin removal efficiencies in both GMF and MF/UF processes.

Dissolved marine algal toxins rejection rates by the RO membrane have been reported by Laycock and co-workers [8] and Seubert and co-workers [10] in laboratory and pilot scale studies. The removal

efficiencies for RO ranged from 99.0 to >99.9% for all toxins studied (Table 2) (see Supplementary Materials, Section 3.5 and Table S9 for additional validation). It is important to note that 100% removal was not assumed in this study as the analytical detection limits ranged from 0.1, 0.2–0.5, to 0.02 ($\mu\text{g/L}$) for OA, DA, and STX, respectively. Thus, the analytical methods used in these studies were not able to detect trace masses of these toxins in the sub-micron to nanogram range or lower [8,10]. Uniform probability distributions were used to sample the range of dissolved toxin removals across the RO membranes.

2.4. pMFA Simulation Algorithm

A Monte Carlo based simulation method was the main approach for the pMFA using 10,000 iterations per run to achieve statistical rigor [49]. The algorithm developed to run the simulations was based on the following procedure using MATLAB (*Mathworks Inc.*, Natick, MA, USA, r2015b): (1) randomly sample the system input of toxins (intracellular and dissolved), toxin removal and generation (from cell breakage) efficiency of each treatment processes from the prior initial distribution; (2) run the pMFA model using this unique combination of toxin input and plant operation efficiency; (3) store the output concentration of toxins in the permeate water and backwash/brine water; (4) repeat this process using a different draw of initial toxin input and operation efficiency from the prior distribution until the number of iterations had been reached.

2.5. Statistical and Sensitivity Analysis

A one-way analysis of variance (ANOVA) was conducted to assess the statistical significance of the results from the pMFA simulations for toxin concentration distributions (TCDs) in both the permeate and combined backwash/brine water. The one-way ANOVA specifically tested the hypothesis of whether the means of the resulting posterior probability distributions were equal (assuming the TCDs were normally distributed). A Tukey honestly significant difference post hoc analysis method was further incorporated to assess the statistical significance of the data (for significant ANOVA outcomes only) by comparing individual means of toxin concentration from different pretreatment trains using variables from the ANOVA output.

A sensitivity analysis was conducted to determine which environmental inputs and treatment efficiencies were the most influential contributors to the predicted posterior TCDs, both in the permeate and backwash/brine waters. The sensitivity analysis was separated into two categories: (a) the sensitivity of the pMFA simulations related to the environmental inputs and (b) the sensitivity of the model related to the treatment efficiencies [17,18,49,50]. The rank of importance was developed for both environmental input and treatment efficiency to assess the confidence in the model through comparison of sensitivity and relative order of uncertainty [17,18]. The sensitivity of the posterior toxin distribution related to each removal efficiency or environmental input was calculated using Equation (9) [17,18].

$$S = \left[\frac{\frac{\Delta X_{mean}}{X_{mean}}}{\frac{\Delta P_{mean}}{P_{mean}}} \right] * \sigma \quad (9)$$

S is the sensitivity value (unitless), σ is the standard deviation of original environmental input or removal efficiency values, X_{mean} is the mean of the posterior toxin distribution in the permeate waters using the original values, ΔX_{mean} is the difference in means between the original posterior distribution and the changed posterior distribution, P_{mean} is the mean of the original prior data probability distribution, and ΔP_{mean} is the difference in means between the original prior probability distribution and the changed prior probability distribution.

2.6. Determination of Human Health Risks from Marine Algal Toxins

A quantitative chemical risk assessment was conducted by incorporating the predicted concentrations of algal toxins remaining in permeate waters following U.S. Environmental Protection

Agency (EPA) guidelines [51]. Human exposure to the algal toxin through ingestion of desalinated water was evaluated through daily intake rate established by U.S. EPA guidelines [51].

Since all of the target toxins display acute toxicity in humans, a thresholding effect based on acute reference doses (*RfD*) was used. Although *RfD*s have been established for shellfish by the U. S. Food & Drug Administration and European Food Safety Administration (EFSA), the relevance of these doses may not carry equal weight when applying them to drinking water exposure scenarios. For drinking water purposes, we re-analyzed the *RfD*s for shellfish consumption, assuming the same LOAEL (lowest observed adverse effect level) or NOAEL (no observed adverse effect level) and uncertainty factors widely used in the shellfish *RfD* calculations by the EFSA [52] (see Supplementary Materials, Section 4 for a complete derivation of *RfD* values).

From the estimated *RfD*s, an acceptable level (*AL*, also known as a maximum contaminant level goal) of each toxin in drinking water was calculated using the *RfD*, body weight (*BW*, 70 kg), relative source contribution (*RSC*), and drinking water intake rate (*IR*, 2 L/day) (Equation (10), [53,54]). A complete derivation of *AL* values can be found in the Supplementary Materials (Section 4).

$$AL = \frac{RfD * BW * RSC}{IR} \quad (10)$$

The *RSC* represents the relative expected contribution of exposure from drinking water compared to other potential routes of exposure, in which the recommended range is between 0.2 and 0.8 [55]. For this study, we chose a conservative value of 0.5 to equally account for other potential routes of exposure other than drinking water such as ingestion of algal toxins in shellfish or fish.

A quantitative estimate of the relative risk of acute human illness was further evaluated using a calculated margin of safety (*MO*) (*AL* normalized by the concentration of algal toxin predicted in the permeate water) [56,57]. A range in *MO*s was calculated using one standard deviation confidence intervals of the mean toxin concentration in the permeate water. *MO*s greater than 1 indicated that the relative risk was low, where higher *MO*s (>1000) suggested that the relative risk was minimal to none [56,57].

3. Results

3.1. Comparison of Algal Toxin Removal Efficiencies

The pMFA model outputs indicated TCDs followed normal probability distribution in RO permeates for all pretreatment train configurations. STX concentration distributions were shown as representations for all other toxins (Figure 2). These normal probability TCDs were the basis of comparison for the removal efficiency of various pretreatment configurations.

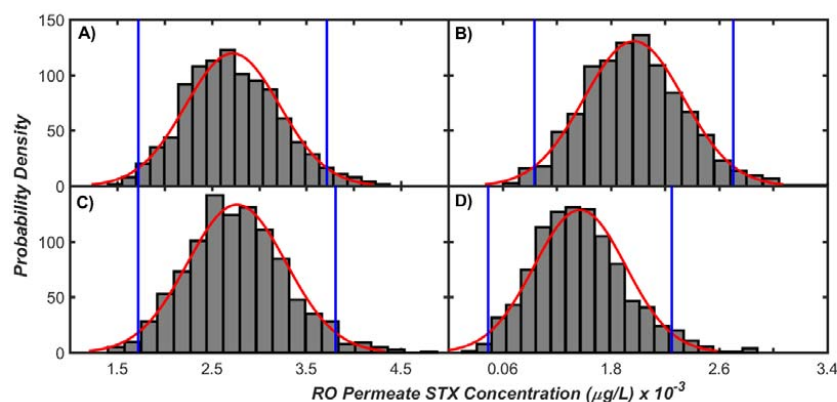


Figure 2. STX toxin concentrations in the RO permeate for: (A) GMF processes without coagulation (*T8*); (B) Pressurized MF/UF processes without coagulation (*T9*); (C) GMF processes with coagulation (*T6*); and (D) Pressurized MF/UF processes with coagulation (*T4*).

The pMFA results demonstrated that a low, but detectable quantity, of algal toxins was present in the permeate water, despite 99.0–99.9% removal across the RO membranes. Concentrations of DA in the permeate were the most significant out of all algal toxins, ranging from 0.5 to 2.8 $\mu\text{g/L}$, whereas concentrations of STX were considerably lower (1–5 ng/L) (Figure 3). Despite the differences in concentrations observed, the risk of acute intoxication from STX is comparable in magnitude to DA due to the dramatic difference in toxicities of each compound (which are further discussed in Section 3.3).

In general, MF/UF pretreatment processes with coagulation/DAF outperformed the toxin removal by GMF processes, with mean toxin removal efficiencies ranging from 47 to 57% (Figure 3). This performance depended on whether the MF/UF pretreatment processes included coagulation practices as coagulation greatly improved the toxin removal for all GMF pretreatment trains (Figure 3).

Treatment processes without coagulation (for both MF/UF and GMF) demonstrated relatively large treatment variability, as noted by the large interquartile ranges and increased number of outliers from these results (Figure 3). Again, reliable treatment performances (represented by low statistical variability) were observed for both MF/UF and GMF systems with coagulation (Figure 3).

Submerged MF/UF systems demonstrated a slightly improved treatment performance as compared to pressurized MF/UF systems when comparing the means of the TCDs in the permeate water. The treatment variability of both processes, however, was equivalent and overlapping (Figure 3). Similarly, adding a DAF process for most MF/UF systems was redundant, as the treatment performance and variability for MF/UF systems with and without DAF (with coagulation) were nearly identical for all toxin types.

The concentrations of each algal toxin in the combined backwash/brine waters were higher in magnitude than those observed in both the inlet and permeate waters (Figure 3). Similar to the permeate water, DA concentrations in the backwash/brine waters were the highest in magnitude among all toxin types, ranging from 400 to 1200 $\mu\text{g/L}$ (0.4 to 1.2 mg/L), followed by YTX with concentrations ranging from 100 to 550 $\mu\text{g/L}$. OA and STX concentrations in the backwash/brine waters were much lower in magnitude for all pretreatment process, ranging from 5 to 20 $\mu\text{g/L}$ and 1 to 7 $\mu\text{g/L}$, respectively. The range in toxin concentration of the combined brine/backwash waters increased considerably (at least 2 to 10 times more concentrated) compared to the inlet range in toxin concentration, which greatly depended on the treatment train configuration (see Supplementary Materials Figures S8 and S9).

The reduction in toxicity of the permeate waters for both GMF/MF/UF treatment processes employing coagulation corresponded to an appreciable increase in toxicity of the backwash/brine waters (Figure 3). Submerged vacuum MF/UF systems (with and without coagulation/DAF) resulted in the lowest magnitude of TCDs in the backwash/brine waters for all toxin types, followed by pressurized MF/UF and GMF systems (Figure 3). Similar to the observation for permeate waters, the inclusion of a DAF system had a negligible effect on TCDs in the combined backwash/brine waters (Figure 3).

The variability of the TCDs in the backwash/brine waters was slightly lower for GMF systems employing coagulation compared to systems without coagulation, slightly higher for pressurized MF/UF systems (with and without coagulation), and relatively unchanged for vacuum MF/UF systems (with and without coagulation) (Figure 3). These trends were summarized using all toxin types by examining absolute changes in COV values. In addition, these trends described above were apparent when comparing the interquartile ranges (IQRs) for OA and YTX toxins among the treatment configurations for pressurized and vacuum MF/UF systems, and the IQRs for STX among configurations for GMF systems with and without coagulation (Figure 3, Panels B vs. C). The variation for STX toxins in the backwash/brine waters was high under pressurized GMF systems (T7, Figure 3). Additional results of algal TCDs, toxin concentration factors in backwash and brine reject are presented in Supplementary Materials Sections 5.1–5.3 and in Figures S8–S10.

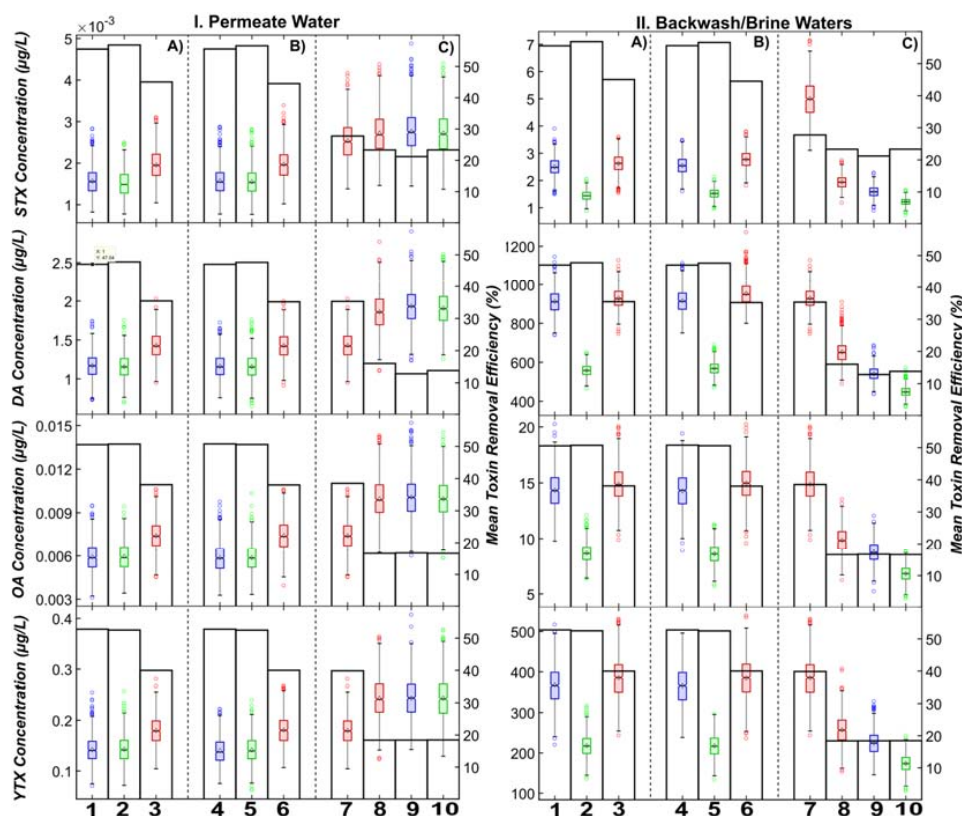


Figure 3. Toxin concentrations (colored box and whisker plot) in the I. Permeate Water and II. Backwash/Brine Waters for all treatment trains (labeled 1–10 for train $T1$ – $T10$). Results are grouped into trains employing (A) DAF; (B) Coagulation; and (C) No Coagulation. Blue, green and red colors represent trains including pressurized MF/UF, vacuum MF/UF, and GMF treatment processes, respectively. The secondary y-axis portrays the mean toxin removal efficiency (shown as open bars) predicted for each treatment train.

The one-way ANOVA demonstrated an overall significant difference in the means of the TCDs in the permeate water resulting from 10 pretreatment train configurations (overall $p < 0.05$). Similarly, the TCDs in the backwash/brine water from 10 treatment processes were all significantly different (overall $p < 0.05$). The overall results for the one-way ANOVA were equivalent for all toxin types (STX, DA, OA, YTX) for both the permeate and backwash/brine waters.

Varying results were obtained for the comparison of individual TCDs in the permeate and backwash/brine waters from different pretreatment processes (p values ranged from <0.05 to 1) (Figure 4). Significant differences were identified when comparing treatment trains with and without coagulation ($p < 0.05$), and trains of no-coagulation vs. those with DAF systems ($p < 0.05$). However, for all processes and most toxins, there was generally not a significant difference in TCDs from processes employing coagulation vs. DAF systems (average $p > 0.1$) (Figure 4).

Significant differences were also identified when comparing across all GMF vs. MF/UF trains ($p < 0.05$) (Figure 4). However, the comparison across all pressurized vs. vacuum driven MF/UF systems did not yield statistically significant outcomes ($p > 0.1$) for most toxins. A “within” treatment comparison of trains employing GMF (i.e., $T3$ vs. $T6$ vs. $T7$ vs. $T8$), or pressurized MF/UF ($T1$ vs. $T4$ vs. $T9$), or vacuum driven MF/UF ($T2$ vs. $T5$ vs. $T10$) revealed a large variability of p values, with values mostly below the 0.05 statistically significant threshold (Figure 4). The p values for all the pairwise comparisons are presented in the Supplementary Materials as well as a complementary figure summarizing the Tukey post hoc comparison tests for the backwash/brine waters (Section 6, Table S11, Figure S11).

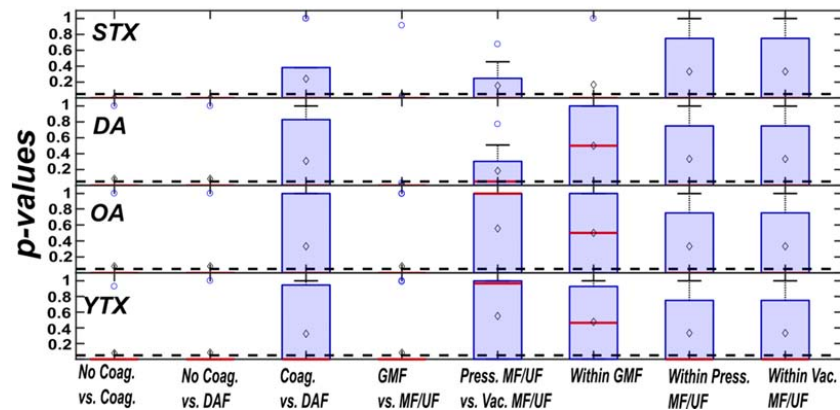


Figure 4. Box and whisker plots of p -values summarizing the Tukey post hoc comparison tests for the permeate waters categorized by each toxin (i.e., STX, DA, OA, YTX). The black dashed lines illustrate the significance level (0.05), while the red lines and black diamonds indicate the median and mean of p -values for each group, respectively. Open circles represent outlying p -values from each comparison group.

3.2. Sensitivity Analysis

Of the model inputs included in the pMFA, the output TCDs were most sensitive to the input algal cell concentration and far less sensitive to the dissolved toxin concentration and intracellular toxin concentration per algal cell (Figure 5A). Dissolved YTXs was the only examined toxin contributing to a noticeable fraction of model sensitivity, ranging from 12 to 14% of the model outcomes (Figure 5A).

The most sensitive parameters for toxin removal efficiency varied according to the pretreatment configuration (Figure 5B). Algal cell removal efficiencies were more sensitive parameters for GMF (T_3, T_6, T_7, T_8) processes as compared to MF/UF ($T_1, T_2, T_4, T_5, T_9, T_{10}$) processes. Contrarily, the resulting TCDs from MF/UF processes were largely affected by the dissolved toxin removal and algal cell breakage parameters over all other removal efficiency parameters for all toxin types (Figure 5B).

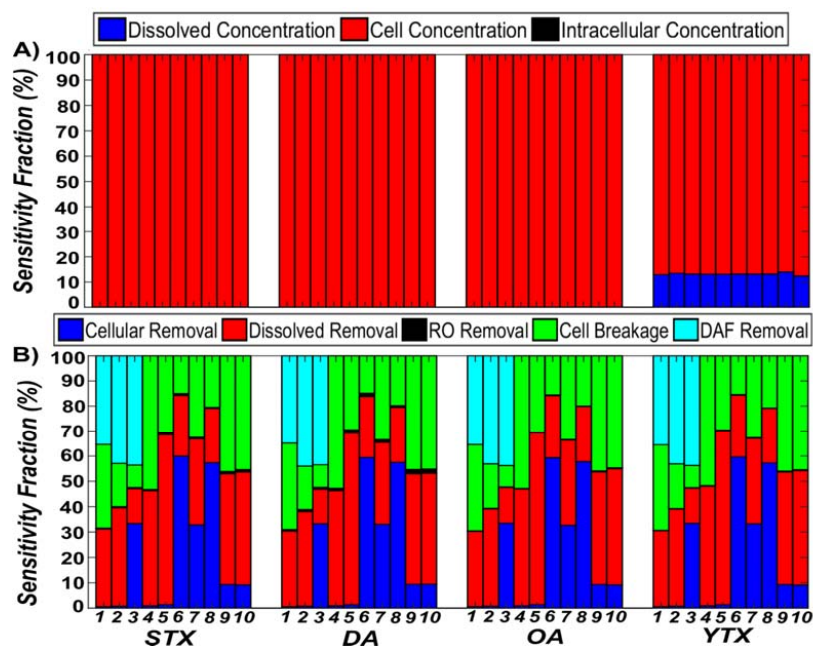


Figure 5. Sensitivity fractions of (A) model inputs; and (B) removal efficiency parameters as a function of algal toxin type and pretreatment processes (labeled as 1–10 for treatment train T_1 – T_{10}).

3.3. Acute Human Health Risks

Acute human health risks were assessed by comparing the calculated AL in drinking water to cumulative probability distributions (CDF) of effluent toxin concentrations in the permeate water. The ALs for STX, DA, OA, and YTX in drinking water were 3.32, 525, 1.40, and 292 $\mu\text{g/L}$, respectively. The simulation results proved that the simulated CDF would never exceed the prescribed AL threshold, based on the acute *RfD* (Figure 6). The tight confidence intervals for these CDF estimates indicated that the certainty in these estimates was high (data not shown). Therefore, the pMFA results demonstrated that the human health risk from ingesting permeate water during algal bloom periods was minimal to none, with greater than 95% certainty. This conclusion is confirmed when comparing the tabulated MO values for each pretreatment process (Figure 6A). All of the MO values are above 1, indicating that there was minimal risk present when consuming permeate water during algal bloom periods (Figure 6A).

The low magnitude of the MO for OA toxins, however, showed that OA toxins contribute most to the drinking water risk during bloom periods in Southern California, followed by DA, YTX, and STX, respectively (Figure 6). This result may seem counterintuitive at first given that the DA toxin loading to the facility is the highest out of all algal toxins, and is the most sparingly removed toxin during pretreatment and across the RO membranes. However, a much lower acute *RfD* (about four orders of magnitude) and AL in the permeate water were estimated for OA as compared to DA. Comparably, the difference in permeate toxin concentrations predicted by the pMFA simulation were only about 2 orders of magnitude different. Therefore, due to the larger difference in acute *RfD* values between the toxins, the acute *RfD* was the most influential parameter affecting risk calculations, resulting in a higher risk for toxins that are less prevalent in Southern California’s coastal waters.

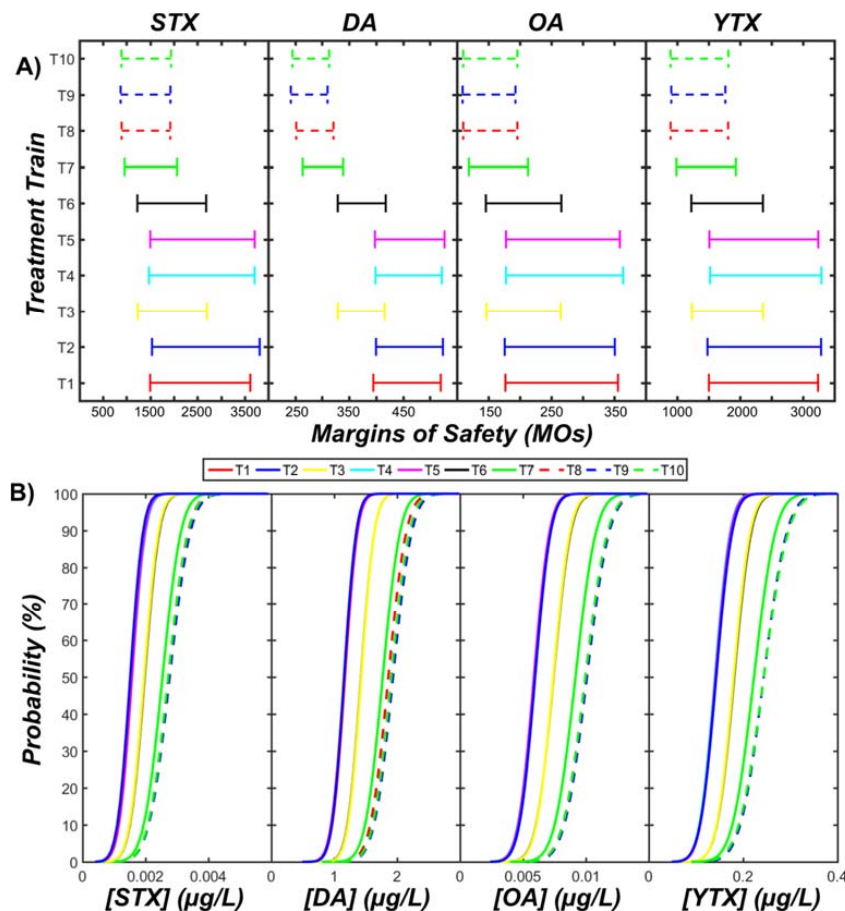


Figure 6. Summary of (A) margins of safety for various algal toxins in the permeate water and (B) cumulative probability distributions of toxin concentrations in the permeate water.

4. Discussion

4.1. Contribution of the Study

This study is the first attempt to estimate marine algal toxin concentrations in the permeate water and combined brine/backwash waters from a full-scale SWRO facility. The removal of algal toxins in full-scale pretreatment systems is important because desalination plant managers and designers can directly benefit from reduced toxin loadings to the RO membranes. Since complete (100%) removal of algal toxins by RO treatment is rarely achieved in full-scale practice, reduction of the toxin loadings reaching the RO membranes can significantly decrease the toxin concentrations in the permeate water and the associated human health risks. To illustrate this point, we compare the operation of a hypothetical situation where a “baseline” pretreatment system is not optimized for toxin removal against the performance of an “optimal” pretreatment configuration presented herein. For the baseline system, if we considered minimal to no removal of DA during pretreatment and 99% RO removal efficiency, a concentration of 200 µg/L of DA in the inlet would result in 2 µg/L in the permeate, which translates to an MO of 263. If, however, we assumed an optimal pretreatment system removing 57% DA before reaching the RO membrane, the new MO (610), or the risk of acute illness from ingesting produced water, would be reduced by a factor of approximately 2.

Another potential benefit of optimizing pretreatment practices for marine biotoxin removal is to avoid toxin breakthrough across the RO membrane due to changes in the RO toxin removal efficiency over time. In full-scale practice, it is likely that the RO toxin removal efficiency will vary over the course of operation due to changes in RO membrane properties and feed water composition. For example, formation of a fouling layer on the surface of RO membranes during operation may alter toxin transport, especially for the small molecular weight and polar (more hydrophilic) toxins DA and STX [58–60]. Cake enhanced concentration polarization, charge interactions, or other mechanisms may lead to increased or decreased rejection of these toxins, depending on the concentration of the toxins in the feed water, the physico-chemical characteristics of the toxins, the membrane (i.e., pore size, hydrophobicity, etc.), as well as the extent and type of membrane fouling [60]. In addition, high concentrations of these toxins on the RO membrane surface may serve as exogenous carbon and nutrient sources for bacteria escaping pretreatment processes, potentially intensifying the biofouling potential of the RO membranes [61].

Although the primary purpose of SWRO pretreatment is to remove excess turbidity, TSS, microorganisms and TOC for RO membrane fouling protection, this study has demonstrated that the SWRO pretreatment selection, design, and operation can have a significant impact on the removal of algal biotoxins. STX, DA, OA, and YTX removal efficiencies were subject to variation, ranging from 15 to 57% for all algal toxins and pretreatment processes. The predicted removal efficiencies (up to 57%) accounted for nearly one quarter to one half of the overall removal of algal biotoxins, where the other three quarters to one half of removal can be accounted for by the RO membranes. The fraction of toxin removal predicted by the pMFA during pretreatment was higher than initially expected, especially for pretreatment processes not designed to target the removal of these toxins. These results suggest that modifications to the operations of SWRO pretreatment processes, rather than the design, could have the most pragmatic and far-reaching impacts on biotoxin removal. Amendments to plant operations, such as coagulant addition, would not hinder but provide additional benefits other than toxin removal, such as removal of TSS, other colloidal particles, and dissolved organic matter. The most significant proof to this supposition was the magnitude of change observed between all systems (both GMF and MF/UF) operating with and without coagulation and the statistically significant differences in TCDs in the permeate or backwash waters both among and within these treatment trains. In both GMF and MF/UF systems, coagulation was critical to (1) reduce the variability in permeate TCDs and (2) increase the magnitude of mean toxin removal efficiencies.

Another potential operational change considered in this study was to assess the operation of MF/UF systems at lower transmembrane pressures in submerged configurations. Although submerged

MF/UF systems (<0.4 bar) had higher mean toxin removal efficiencies and lower variability in treatment than the pressurized systems (>0.4 bar), the TCDs in the permeate and backwash waters were not significantly different between the systems. Therefore, the selection of submerged systems over pressurized systems in pretreatment design for biotoxin mitigation may not be as critical as expected initially.

Amending the design of the SWRO pretreatment system with a DAF system demonstrated mixed results from the pMFA simulations regarding toxin removal efficiencies. On one hand, statistically significant reductions in TCDs were observed for DAF systems compared to systems operating without coagulation, whereas no statistically significant differences were found between systems operating with DAF and those with coagulation. It was likely that the above discrepancies observed in the results of the pMFA were due to: (1) the high variability of reported removal efficiencies of algal cells in DAF systems (i.e., 43–93%) and (2) the scarcity of studies (N = 3) examining algal cell removal in DAF systems [42,47,48]. The high variability in reported algal removal efficiencies from DAF systems results directly from the site specific algal species composition during the evaluation period for each study [12]. Voutchkov [12] stated that removal of chlorophyll-a is often lower for DAF treatment systems as most of the influent water (up to 50–75% at the intake) comprises picoplankton, which are sparsely removed by DAF processes. Future studies should consider reporting both reductions in chlorophyll-a and algal species profiles as determined by microscopy for standardizing their reported results. An equally important aspect to consider in future study (that was neglected in this study) is the removal of dissolved toxins in DAF systems. Previous studies have indicated considerable biopolymer and humic acid removal in these systems [12,42,48]; therefore, the removal of other soluble organics, such as algal toxins, would greatly improve the accuracy of future pMFA simulations.

Future design of pretreatment systems and configurations should consider the impact of HAB periods on plant operations. The results highlighted a great difference in treatment potential between GMF and MF/UF systems, with MF/UF systems demonstrating improved performances. This difference in performance was attributed to the high range in algal cell removal and small cell removal variability reported in the literature for MF/UF processes. Subpar removal of algal biotoxins by GMF systems can be attributed to the colloidal size of most marine microalgae associated with harmful algal bloom periods. Most conventional sand filtration media has an effective size range of 0.4 to 0.6 mm (400 to 600 μm), which is much larger than the corresponding width and length dimensions of dinoflagellates and diatoms (10 to 100 μm) [1]. Marine microalgae are negatively charged and may not adsorb to the negatively charged surface of the filter media or organic material already adsorbed to the grain surface. Similarly, the high filtration rates often applied during GMF may prevent the conglomeration and straining of algal cells.

It is also necessary to consider the differences in dissolved toxin removal for both GMF and MF/UF processes in the future. Using more hydrophobic membranes has proven to increase adsorption of algal toxins, including MC-LR, through partitioning of these toxins based on phase affinity of the membrane surface [62–64]. Equally critical is the potential for dissolved toxin adsorption (mainly by electrostatic interactions) to or phase affinity for the compressible organic cake layer formed at the surface of the membrane [44,65].

Potential benefits of GMF systems—such as increased biological activity—may increase the removal of dissolved toxins over MF/UF systems. Voutchkov [1] has stated that the removal of soluble organics in some second stage GMF systems can account to 20–40% by biological filtration processes alone. Biological treatment has the potential to remove dissolved organic carbon and TEP of the source water without requiring expensive cleaning/purchase of coagulants or cleaning chemicals, energy intensive backwashing (increase in filter run times), and can reduce the replacement frequency of membranes over the duration of operation [39,40,66–68].

Other than pretreatment design and operation, the design of a proper seawater intake system represents a significant amendment for future SWRO facilities to mitigate the effects of HABs [12–14]. Although a majority of current SWRO facilities operate with an open (surface water) intake system,

the use of subsurface systems (wells and galleries) can significantly reduce the influent suspended solids, bacteria, dissolved organic carbon, and toxic/non-toxic algae present in the source water [69,70]. Subsurface intakes are well suited for coastal regions where the geology is favorable (i.e., the presence of permeable rocks, limestones, dolomites or gravels), which may limit the widespread application of these intake systems to future SWRO facilities intending to alleviate the deleterious effects of HABs [70].

4.2. Uncertainty and Variability

Since there is little experimental data to verify the effluent pretreatment concentrations predicted by the pMFA, a certainty/variability analysis was performed to elucidate the accuracy of the model predictions. Algal breakage fractions represented the highest model uncertainty. The algal cell breakage fractions were informed estimates made by extrapolating experimental data summarized in Voutchkov [12]. However, algal cell breakage behavior is influenced not only by operational practices (shear in pumps or valves, transmembrane pressure), but also algal cell type and species (diatom or dinoflagellates) and other biotic factors such as cell age [71–77]. We reduced this high uncertainty in our model by structuring the distribution of breakage coefficients to encompass a relatively large range, and by incorporating uniform probability distributions for selecting breakage coefficients during each simulation.

The dissolved toxin removal coefficients were also subject to a moderate to high uncertainty when extrapolating from MC-LR observations summarized from the literature. This extrapolation was based on the octanol-water distribution coefficients either experimentally derived or modeled from molecular structure alone (see Supplementary Materials Section 3.1). We focused primarily on collecting experimental observations of octanol water distribution coefficients over modelled predictions to first reduce the relative uncertainty in dissolved toxin removals. In addition, we focused on collecting field and pilot studies examining the dissolved removal of MC-LR over laboratory studies to further reduce the uncertainty of pMFA simulations.

The sensitivity results indicated that algal cell removal was the most sensitive parameter for GMF systems, whereas dissolved toxin removal and algal cell breakage were the most sensitive parameters for MF/UF systems. Given these results, there is higher certainty in the GMF simulations over the MF/UF simulations. However, if we analyze the entire system, the algal cell concentration was the most sensitive input. When model inputs were grouped with the removal efficiency parameters in the sensitivity analysis, greater than 99% of the model output still depended on the algal cell concentration alone (data not shown). This is a significant conclusion given that the uncertainty of the algal cell concentration is low compared to all other model inputs or parameters. Based on this result, the model predictions can be afforded relatively high levels of confidence, despite the uncertainty observed for some of the model removal efficiency parameters.

To improve the pMFA model predictions, several areas of data collection should be improved and prioritized. The first and foremost step would be to collect algal toxin data from a full-scale SWRO facility at different points in the treatment train for a prolonged time period (i.e., 3 years). This data collection effort would allow a clear comparison between pMFA model predictions and real-world data, potentially providing the opportunity to optimize removal efficiency parameters and compare these removal efficiency estimates to those observed in practice. Ultimately, from this data collection, a true quantitative estimate of the certainty of model predictions can be reached. An additional area of research would be to study the algal cell breakage magnitude for different pretreatment configurations during various stages of algal blooms and analyzing the dissolved removal of algal toxins during various pretreatment processes. This study extrapolated treatment efficiencies of dissolved toxins from MC-LR removal data, based on similarity or differences in physical and chemical properties. The new research should be integrated with the field data collection effort to develop an improved understanding of toxin removal during SWRO pretreatment.

4.3. Human Health Effects

The lifetime risk of acute human illness from ingesting permeate waters during algal blooms was determined to be minimal using a quantitative chemical risk assessment framework. The AL was determined based on the acute *RfD* developed by the EFSA. Most of these doses (STX, DA, OA) were based on LOAEL from actual human shellfish poisoning events, and should be more reliable than animal testing data (YTX). In addition, the *RfD* developed by the EFSA considered two to three uncertainty factors (extrapolating from LOAEL to NOAEL, accounting for intra-species variation), depending on the toxin, which further decreases the margin of acceptable risk. Based on these facts, we are confident in the human health effect conclusions presented in this study.

Although we have thoroughly addressed the acute human health risks from exposure to algal toxins, the chronic, accumulated, or compounding human health risks associated with exposure to low levels of these toxins in desalinated drinking water are relatively unknown. For example, several studies have indicated that repetitive exposure to low level doses of OA through shellfish consumption may be correlated to an increase in the incidence of colorectal cancers in exposed human populations [78–80]. Developmental and neurological effects of chronic (low-level) DA exposure on infants and young children are a concern, as DA has been shown to cross the placenta, enter the blood brain barrier of infants, and collect in amniotic fluid in mammals [81–85]. Chronic DA exposure has also been linked to cognitive impairment in mice [86]. More reliable chronic DA exposure epidemiological studies on humans, however, have been rarely reported. A recent study by Grattan and co-workers concluded that there was a possible, but not clinically significant, connection between long term, low level exposure to DA (through razor clam consumption) and memory [87]. Future studies should consider the development of chronic *RfDs* of algal biotoxins in desalinated drinking water for lifetime exposure human health risk assessments.

The effect of concentrated brine and backwash waters on both human health and the surrounding environment during harmful algal bloom periods should be a topic of equal concern for future study, as the results from pMFA simulations indicated a relatively high concentration of algal biotoxins in the combined backwash/brine waters (up to mg/L levels). Besides ingestion of finished drinking water, humans may be at risk when exposed to elevated concentrations of algal biotoxins either through recreational exposure pathways or consumption of contaminated seafoods. The ingestion of contaminated shellfish harvested near the zone of dilution at the desalination brine discharge point may pose the most critical human health risk, as benthic shellfish are chronically exposed to elevated concentrations of biotoxins from the combined backwash/brine discharge. An important question would be to assess whether the background concentration of dissolved toxin during HAB periods contributes more to shellfish bioaccumulation than the actual SWRO discharge itself. Studies should equally weigh the potential biomagnification of algal biotoxins in the surrounding ecosystem as another environmental issue emanating from concentrated SWRO brine discharge.

5. Conclusions

The primary objective of this study was to quantify the removal of algal toxins during SWRO using a pMFA approach. The main conclusions drawn from this study are:

- A detectable quantity of algal toxins is present in the permeate water, despite almost 99.0–99.9% removal predicted across the RO membranes (in the ng/L to µg/L range);
- A relatively high concentration of algal toxins was predicted for the combined backwash and RO reject waters (in the µg/L to mg/L range);
- MF/UF systems with coagulation generally had the highest predicted toxin removals (and least variability) over all GMF systems/operations (up to 57% of the entire removal across SWRO);
- There is a low to negligible risk of acute intoxication from ingesting desalinated water during algal bloom periods (margins of safety ranged from 100 to 4000).

Supplementary Materials: The Supplementary Materials are available online at www.mdpi.com/2073-4441/9/10/730/s1. Investigation of Algal Biotxin Removal during SWRO Desalination through a Materials Flow Analysis.

Acknowledgments: The authors acknowledge Southern California Coastal Ocean Observing System for coastal water monitoring data and UCI Ocean for support of this study.

Author Contributions: Derek Manheim conceived, designed, and carried out the analysis of the pMFA simulations and wrote the manuscript; Sunny Jiang contributed to the study design, the model development, data presentation and analysis, and the writing of the manuscript.

Conflicts of Interest: The authors declare no conflict of interest.

Abbreviations

SWRO	Seawater Reverse Osmosis
RO	Reverse Osmosis
HABs	Harmful Algal Blooms
pMFA	Probabilistic Materials Flow Analysis
MF/UF	Microfiltration/Ultrafiltration
GMF	Granular Media Filtration
DAF	Dissolved Air Flotation
TEP	Transparent Extracellular Particulate
MGD	Million Gallons per Day (international unit)
SCCOOS	Southern California Coastal Ocean Observing System
STX	Saxitoxin
DA	Domoic Acid
OA	Okadaic Acid
YTX	Yessotoxin
ECDF	Empirical Cumulative Distribution Function
SPATT	Solid Phase Adsorption Toxin Tracking
MC-LR	Microcystin-LR
ANOVA	Analysis of Variance
RfD	Acute Reference Dose
EFSA	European Food Safety Administration
EPA	Environmental Protection Agency
AL	Acceptable Level
LOEL	Lowest Observed Effect Level
NOAEL	No Observed Adverse Effect Level
RSC	Relative Source Contribution
MO	Margin of Safety
TCD	Toxin Concentration Distribution
IQR	Interquartile Range
COV	Coefficient of Variation
CDF	Cumulative Probability Distribution Functions

References

1. Voutchkov, N. *Desalination Engineering: Planning and Design*; McGraw Hill Professional: New York, NY, USA, 2011.
2. Dawoud, M.A. The role of desalination in augmentation of water supply in GCC countries. *Desalination* **2005**, *186*, 187–198. [[CrossRef](#)]
3. Ghaffour, N.; Missimer, T.M.; Amy, G.L. Technical review and evaluation of the economics of water desalination: Current and future challenges for better water supply sustainability. *Desalination* **2013**, *309*, 197–207. [[CrossRef](#)]
4. Schiffler, M. Perspectives and challenges for desalination in the 21st century. *Desalination* **2004**, *165*, 1–9.
5. Eltawil, M.A.; Zhengming, Z.; Yuan, L. A review of renewable energy technologies integrated with desalination systems. *Renew. Sustain. Energy Rev.* **2009**, *13*, 2245–2262. [[CrossRef](#)]

6. Subramani, A.; Badruzzaman, M.; Oppenheimer, J.; Jacangelo, J.G. Energy minimization strategies and renewable energy utilization for desalination: A review. *Water Res.* **2011**, *45*, 1907–1920. [[CrossRef](#)] [[PubMed](#)]
7. Ghaffour, N.; Missimer, T.M.; Amy, G.L. Combined desalination, water reuse, and aquifer storage and recovery to meet water supply demands in the GCC/MENA region. *Desalination Water Treat.* **2013**, *51*, 38–43. [[CrossRef](#)]
8. Laycock, M.V.; Anderson, D.M.; Naar, J.; Goodman, A.; Easy, D.J.; Donovan, M.A.; Li, A.; Quilliam, M.A.; Al Jamali, E.; Alshihhi, R. Laboratory desalination experiments with some algal toxins. *Desalination* **2012**, *293*, 1–6. [[CrossRef](#)]
9. Boerlage, S.; Nada, N. Algal toxin removal in seawater desalination processes. *Desalination Water Treat.* **2015**, *55*, 2575–2593. [[CrossRef](#)]
10. Seubert, E.L.; Trussell, S.; Eagleton, J.; Schnetzer, A.; Cetinić, I.; Lauri, P.; Jones, B.H.; Caron, D.A. Algal toxins and reverse osmosis desalination operations: Laboratory bench testing and field monitoring of domoic acid, saxitoxin, brevetoxin and okadaic acid. *Water Res.* **2012**, *46*, 6563–6573. [[CrossRef](#)] [[PubMed](#)]
11. Caron, D.A.; Garneau, M.-È.; Seubert, E.; Howard, M.D.A.; Darjany, L.; Schnetzer, A.; Cetinić, I.; Filteau, G.; Lauri, P.; Jones, B.; et al. Harmful algae and their potential impacts on desalination operations off southern California. *Water Res.* **2010**, *44*, 385–416. [[CrossRef](#)] [[PubMed](#)]
12. Voutchkov, N. Considerations for selection of seawater filtration pretreatment system. *Desalination* **2010**, *261*, 354–364. [[CrossRef](#)]
13. Villacorte, L.O.; Tabatabai, S.A.A.; Dhakal, N.; Amy, G.; Schippers, J.C.; Kennedy, M.D. Algal blooms: An emerging threat to seawater reverse osmosis desalination. *Desalination Water Treat.* **2015**, *55*, 2601–2611. [[CrossRef](#)]
14. Villacorte, L.O.; Tabatabai, S.A.A.; Anderson, D.M.; Amy, G.L.; Schippers, J.C.; Kennedy, M.D. Seawater reverse osmosis desalination and (harmful) algal blooms. *Desalination* **2015**, *360*, 61–80. [[CrossRef](#)]
15. Huang, X.; Min, J.H.; Lu, W.; Jaktar, K.; Yu, C.; Jiang, S.C. Evaluation of methods for reverse osmosis membrane integrity monitoring for wastewater reuse. *J. Water Process Eng.* **2015**, *7*, 161–168. [[CrossRef](#)]
16. Meyerhofer, P.; Desormeaux, E.; Luckenbach, H. *Seawater Reverse Osmosis Desalination Pilot Test Program Report*; Santa Cruz Water District: Santa Cruz, CA, USA, 2010.
17. Gottschalk, F.; Scholz, R.W.; Nowack, B. Probabilistic material flow modeling for assessing the environmental exposure to compounds: Methodology and an application to engineered nano-TiO₂ particles. *Environ. Model. Softw.* **2010**, *25*, 320–332. [[CrossRef](#)]
18. Gottschalk, F.; Sonderer, T.; Scholz, R.W.; Nowack, B. Possibilities and limitations of modeling environmental exposure to engineered nanomaterials by probabilistic material flow analysis. *Environ. Toxicol. Chem.* **2010**, *29*, 1036–1048. [[CrossRef](#)] [[PubMed](#)]
19. California Department of Water Resources (CDWR). *California Water Plan Update 2013: Volume 3-Resource Management Strategies-Chapter 10 Desalination (Brackish and Seawater)*; CDWR: Sacramento, CA, USA, 2013.
20. Seubert, E.L.; Gellene, A.G.; Howard, M.D.A.; Connell, P.; Ragan, M.; Jones, B.H.; Runyan, J.; Caron, D.A. Seasonal and annual dynamics of harmful algae and algal toxins revealed through weekly monitoring at two coastal ocean sites off southern California, USA. *Environ. Sci. Pollut. Res.* **2013**, *20*, 6878–6895. [[CrossRef](#)] [[PubMed](#)]
21. Allen, J.L.; Smyth, T.J.; Siddorn, J.R.; Holt, M. How well can we forecast high biomass algal bloom events in a eutrophic coastal sea? *Harmful Algae* **2008**, *8*, 70–76. [[CrossRef](#)]
22. Kim, H.-J.; Miller, A.J.; McGowan, J.; Carter, M.L. Coastal phytoplankton blooms in the Southern California Bight. *Prog. Oceanogr.* **2009**, *82*, 137–147. [[CrossRef](#)]
23. Schnetzer, A.; Miller, P.E.; Schaffner, R.A.; Stauffer, B.A.; Jones, B.H.; Weisberg, S.B.; DiGiacomo, P.M.; Berelson, W.M.; Caron, D.A. Blooms of *Pseudo-nitzschia* and domoic acid in the San Pedro Channel and Los Angeles harbor areas of the Southern California Bight, 2003–2004. *Harmful Algae* **2007**, *6*, 372–387. [[CrossRef](#)]
24. Trainer, V.L.; Cochlan, W.P.; Erickson, A.; Bill, B.D.; Cox, F.H.; Borchert, J.A.; Lefebvre, K.A. Recent domoic acid closures of shellfish harvest areas in Washington State inland waterways. *Harmful Algae* **2007**, *6*, 449–459. [[CrossRef](#)]
25. Bargu, S.; Powell, C.L.; Wang, Z.; Doucette, G.J.; Silver, M.W. Note on the occurrence of *Pseudo-nitzschia australis* and domoic acid in squid from Monterey Bay, CA (USA). *Harmful Algae* **2008**, *7*, 45–51. [[CrossRef](#)]

26. Lefebvre, K.A.; Bill, B.D.; Erickson, A.; Baugh, K.A.; O'Rourke, L.; Costa, P.R.; Nance, S.; Trainer, V.L. Characterization of Intracellular and Extracellular Saxitoxin Levels in Both Field and Cultured *Alexandrium* spp. Samples from Sequim Bay, Washington. *Mar. Drugs* **2008**, *6*, 103–116. [[CrossRef](#)] [[PubMed](#)]
27. MacKenzie, L.; Beuzenberg, V.; Holland, P.; McNabb, P.; Selwood, A. Solid phase adsorption toxin tracking (SPATT): A new monitoring tool that simulates the biotoxin contamination of filter feeding bivalves. *Toxicon* **2004**, *44*, 901–918. [[CrossRef](#)] [[PubMed](#)]
28. Jester, R.J.; Baugh, K.A.; Lefebvre, K.A. Presence of *Alexandrium catenella* and paralytic shellfish toxins in finfish, shellfish and rock crabs in Monterey Bay, California, USA. *Mar. Biol.* **2009**, *156*, 493. [[CrossRef](#)]
29. MacKenzie, L.; Beuzenberg, V.; Holland, P.; McNabb, P.; Suzuki, T.; Selwood, A. Pectenotoxin and okadaic acid-based toxin profiles in *Dinophysis acuta* and *Dinophysis acuminata* from New Zealand. *Harmful Algae* **2005**, *4*, 75–85. [[CrossRef](#)]
30. Howard, M.D.A.; Silver, M.; Kudela, R.M. Yessotoxin detected in mussel (*Mytilus californicus*) and phytoplankton samples from the U.S. west coast. *Harmful Algae* **2008**, *7*, 646–652. [[CrossRef](#)]
31. Kudela, R.M.; Mioni, C.; Peacock, M.; Schraga, T.; Senn, D. *Assessing SPATT in San Francisco Bay*; SFEI Contract 1051 Final Report; University of California, Santa Cruz (UCSC): Santa Cruz, CA, USA, 2015. Available online: <http://sfbaynutrients.sfei.org/sites/default/files/SPATT%20Final%20Report%20May2015.pdf> (accessed on 21 August 2017).
32. Lane, J.Q.; Roddam, C.M.; Langlois, G.W.; Kudela, R.M. Application of Solid Phase Adsorption Toxin Tracking (SPATT) for field detection of the hydrophilic phycotoxins domoic acid and saxitoxin in coastal California. *Limnol. Oceanogr. Methods* **2010**, *8*, 645–660. [[CrossRef](#)]
33. Trainer, V.L.; Bates, S.S.; Lundholm, N.; Thessen, A.E.; Cochlan, W.P.; Adams, N.G.; Trick, C.G. Pseudo-nitzschia physiological ecology, phylogeny, toxicity, monitoring and impacts on ecosystem health. *Harmful Algae* **2012**, *14*, 271–300. [[CrossRef](#)]
34. Graneli, E.; Flynn, K. Chemical and Physical Factors Influencing Toxin Content. In *The Ecology of Harmful Algae*; Graneli, E., Turner, J., Eds.; Ecological Studies; Springer: Berlin/Heidelberg, Germany, 2006; Volume 189, pp. 229–239.
35. Leparc, J.; Rapenne, S.; Courties, C.; Lebaron, P.; Croué, J.P.; Jacquemet, V.; Turner, G. Water quality and performance evaluation at seawater reverse osmosis plants through the use of advanced analytical tools. *Desalination* **2007**, *203*, 243–255. [[CrossRef](#)]
36. Bar-Zeev, E.; Berman-Frank, I.; Liberman, B.; Rahav, E.; Passow, U.; Berman, T. Transparent exopolymer particles: Potential agents for organic fouling and biofilm formation in desalination and water treatment plants. *Desalination Water Treat.* **2009**, *3*, 136–142. [[CrossRef](#)]
37. Sabiri, N.E.; Castaing, J.B.; Massé, A.; Jaouen, P. Performance of a sand filter in removal of micro-algae from seawater in aquaculture production systems. *Environ. Technol.* **2012**, *33*, 667–676. [[CrossRef](#)] [[PubMed](#)]
38. Remize, P.-J.; Laroche, J.-F.; Leparc, J.; Schrotter, J.-C. A pilot-scale comparison of granular media filtration and low-pressure membrane filtration for seawater pretreatment. *Desalination Water Treat.* **2009**, *5*, 6–11. [[CrossRef](#)]
39. Bar-Zeev, E.; Belkin, N.; Liberman, B.; Berman, T.; Berman-Frank, I. Rapid sand filtration pretreatment for SWRO: Microbial maturation dynamics and filtration efficiency of organic matter. *Desalination* **2012**, *286*, 120–130. [[CrossRef](#)]
40. Bar-Zeev, E.; Belkin, N.; Liberman, B.; Berman-Frank, I.; Berman, T. Bioflocculation: Chemical free, pre-treatment technology for the desalination industry. *Water Res.* **2013**, *47*, 3093–3102. [[CrossRef](#)] [[PubMed](#)]
41. Plantier, S.; Castaing, J.-B.; Sabiri, N.-E.; Massé, A.; Jaouen, P.; Pontié, M. Performance of a sand filter in removal of algal bloom for SWRO pre-treatment. *Desalination Water Treat.* **2013**, *51*, 1838–1846. [[CrossRef](#)]
42. Guastalli, A.R.; Simon, F.X.; Penru, Y.; de Kerchove, A.; Llorens, J.; Baig, S. Comparison of DMF and UF pre-treatments for particulate material and dissolved organic matter removal in SWRO desalination. *Desalination* **2013**, *322*, 144–150. [[CrossRef](#)]
43. Campinas, M.; Rosa, M.J. Evaluation of cyanobacterial cells removal and lysis by ultrafiltration. *Sep. Purif. Technol.* **2010**, *70*, 345–353. [[CrossRef](#)]
44. Castaing, J.B.; Massé, A.; Séchet, V.; Sabiri, N.-E.; Pontié, M.; Haure, J.; Jaouen, P. Immersed hollow fibres microfiltration (MF) for removing undesirable micro-algae and protecting semi-closed aquaculture basins. *Desalination* **2011**, *276*, 386–396. [[CrossRef](#)]

45. Frappart, M.; Massé, A.; Jaffrin, M.Y.; Pruvost, J.; Jaouen, P. Influence of hydrodynamics in tangential and dynamic ultrafiltration systems for microalgae separation. *Desalination* **2011**, *265*, 279–283. [[CrossRef](#)]
46. Zhang, Y.; Tian, J.; Nan, J.; Gao, S.; Liang, H.; Wang, M.; Li, G. Effect of PAC addition on immersed ultrafiltration for the treatment of algal-rich water. *J. Hazard. Mater.* **2011**, *186*, 1415–1424. [[CrossRef](#)] [[PubMed](#)]
47. Kim, S.-H.; Min, C.-S.; Lee, S. Application of dissolved air flotation as pretreatment of seawater desalination. *Desalination Water Treat.* **2011**, *33*, 261–266. [[CrossRef](#)]
48. Zhu, I.X.; Bates, B.J.; Anderson, D.M. Removal of *Prorocentrum minimum* from seawater using dissolved air flotation. *J. Appl. Water Eng. Res.* **2014**, *2*, 47–56. [[CrossRef](#)]
49. Finley, B.; Paustenbach, D. The Benefits of Probabilistic Exposure Assessment: Three Case Studies Involving Contaminated Air, Water, and Soil. *Risk Anal.* **1994**, *14*, 53–73. [[CrossRef](#)] [[PubMed](#)]
50. Norton, J.P. Algebraic sensitivity analysis of environmental models. *Environ. Model. Softw.* **2008**, *23*, 963–972. [[CrossRef](#)]
51. Fowle, J.R.; Dearfield, K.L. *Risk Characterization Handbook*; EPA 100-B-00-002; U.S. EPA Science Policy Council: Washington, DC, USA, 2000.
52. Paredes, I.; Rietjens, I.M.C.M.; Vieites, J.M.; Cabado, A.G. Update of risk assessments of main marine biotoxins in the European Union. *Toxicon* **2011**, *58*, 336–354. [[CrossRef](#)] [[PubMed](#)]
53. Cotruvo, J.A. Drinking water standards and risk assessment. *Regul. Toxicol. Pharmacol.* **1988**, *8*, 288–299. [[CrossRef](#)]
54. Donohue, J.; Zavaleta, J.O. Toxicological Basis for Drinking Water Risk Assessment. In *Drinking Water Regulation and Health*; Pontius, F., Ed.; John Wiley & Sons: New York, NY, USA, 2003; pp. 133–146.
55. Howd, R.A.; Brown, J.P.; Fan, A.M. Risk Assessment for Chemicals in Drinking Water: Estimation of Relative Source Contribution. *Toxicologist* **2004**, *78*, 1–10.
56. Cotruvo, J.; Couper, M.; Cunliffe, D.; Fawell, J.; Giddings, M.; Ohanian, E.; Ong, C.N.; Sanderson, H.; Simizaki, D. *Pharmaceuticals in Drinking Water*; World Health Organization: Geneva, Switzerland, 2011.
57. *Water Reuse: Potential for Expanding the Nation's Water Supply through Reuse of Municipal Wastewater*; National Research Council; The National Academies Press: Washington, DC, USA, 2012.
58. Xu, P.; Drewes, J.E.; Kim, T.-U.; Bellona, C.; Amy, G. Effect of membrane fouling on transport of organic contaminants in NF/RO membrane applications. *J. Membr. Sci.* **2006**, *279*, 165–175. [[CrossRef](#)]
59. Ng, H.Y.; Elimelech, M. Influence of colloidal fouling on rejection of trace organic contaminants by reverse osmosis. *J. Membr. Sci.* **2004**, *244*, 215–226. [[CrossRef](#)]
60. Verliefe, A.R.D.; Cornelissen, E.R.; Heijman, S.G.J.; Petrinic, I.; Luxbacher, T.; Amy, G.L.; Van der Bruggen, B.; van Dijk, J.C. Influence of membrane fouling by (pretreated) surface water on rejection of pharmaceutically active compounds (PhACs) by nanofiltration membranes. *J. Membr. Sci.* **2009**, *330*, 90–103. [[CrossRef](#)]
61. Stewart, J.E.; Marks, L.J.; Gilgan, M.W.; Pfeiffer, E.; Zwicker, B.M. Microbial utilization of the neurotoxin domoic acid: Blue mussels (*Mytilus edulis*) and soft shell clams (*Mya arenaria*) as sources of the microorganisms. *Can. J. Microbiol.* **1998**, *44*, 456–464. [[CrossRef](#)] [[PubMed](#)]
62. Lee, J.; Walker, H.W. Effect of Process Variables and Natural Organic Matter on Removal of Microcystin-LR by PAC-UF. *Environ. Sci. Technol.* **2006**, *40*, 7336–7342. [[CrossRef](#)] [[PubMed](#)]
63. Gijsbertsen-Abrahamse, A.J.; Schmidt, W.; Chorus, I.; Heijman, S.G.J. Removal of cyanotoxins by ultrafiltration and nanofiltration. *J. Membr. Sci.* **2006**, *276*, 252–259. [[CrossRef](#)]
64. Lee, J.; Walker, H.W. Mechanisms and factors influencing the removal of microcystin-LR by ultrafiltration membranes. *J. Membr. Sci.* **2008**, *320*, 240–247. [[CrossRef](#)]
65. Babel, S.; Takizawa, S. Microfiltration membrane fouling and cake behavior during algal filtration. *Desalination* **2010**, *261*, 46–51. [[CrossRef](#)]
66. Jeong, S.; Bae, H.; Naidu, G.; Jeong, D.; Lee, S.; Vigneswaran, S. Bacterial community structure in a biofilter used as a pretreatment for seawater desalination. *Ecol. Eng.* **2013**, *60*, 370–381. [[CrossRef](#)]
67. Naidu, G.; Jeong, S.; Vigneswaran, S.; Rice, S.A. Microbial activity in biofilter used as a pretreatment for seawater desalination. *Desalination* **2013**, *309*, 254–260. [[CrossRef](#)]
68. Simon, F.X.; Rudé, E.; Llorens, J.; Baig, S. Study of Seawater Biofiltration by Measuring Adenosine Triphosphate (ATP) and Turbidity. *Water Air Soil Pollut.* **2013**, *224*, 1568. [[CrossRef](#)]

69. Dehwah, A.H.A.; Al-Mashharawi, S.; Kammourie, N.; Missimer, T.M. Impact of well intake systems on bacterial, algae, and organic carbon reduction in SWRO desalination systems, SAWACO, Jeddah, Saudi Arabia. *Desalination Water Treat.* **2015**, *55*, 2594–2600. [[CrossRef](#)]
70. Missimer, T.M.; Ghaffour, N.; Dehwah, A.H.A.; Rachman, R.; Maliva, R.G.; Amy, G. Subsurface intakes for seawater reverse osmosis facilities: Capacity limitation, water quality improvement, and economics. *Desalination* **2013**, *322*, 37–51. [[CrossRef](#)]
71. Vandanjon, L.; Rossignol, N.; Jaouen, P.; Robert, J.M.; Quéméneur, F. Effects of shear on two microalgae species. Contribution of pumps and valves in tangential flow filtration systems. *Biotechnol. Bioeng.* **1999**, *63*, 1–9. [[CrossRef](#)]
72. Hamm, C.E.; Merkel, R.; Springer, O.; Jurkojc, P.; Maier, C.; Prechtel, K.; Smetacek, V. Architecture and material properties of diatom shells provide effective mechanical protection. *Nature* **2003**, *421*, 841–843. [[CrossRef](#)] [[PubMed](#)]
73. Subhash, G.; Yao, S.; Bellinger, B.; Gretz, M.R. Investigation of Mechanical Properties of Diatom Frustules Using Nanoindentation. *J. Nanosci. Nanotechnol.* **2005**, *5*, 50–56. [[CrossRef](#)] [[PubMed](#)]
74. Lasic, D.; Short, K.; Mitchell, J.G.; Lal, R.; Voelcker, N.H. AFM Nanoindentations of Diatom Biosilica Surfaces. *Langmuir* **2007**, *23*, 5014–5021. [[CrossRef](#)] [[PubMed](#)]
75. Lau, R.K.L.; Kwok, A.C.M.; Chan, W.K.; Zhang, T.Y.; Wong, J.T.Y. Mechanical Characterization of Cellulosic Thecal Plates in Dinoflagellates by Nanoindentation. *J. Nanosci. Nanotechnol.* **2007**, *7*, 452–457. [[PubMed](#)]
76. Ladner, D.A.; Vardon, D.R.; Clark, M.M. Effects of shear on microfiltration and ultrafiltration fouling by marine bloom-forming algae. *J. Membr. Sci.* **2010**, *356*, 33–43. [[CrossRef](#)]
77. Michels, M.H.A.; Goot, A.J.; van der Norsker, N.-H.; Wijffels, R.H. Effects of shear stress on the microalgae *Chaetoceros muelleri*. *Bioprocess Biosyst. Eng.* **2010**, *33*, 921–927. [[CrossRef](#)] [[PubMed](#)]
78. Manerio, E.; Rodas, V.L.; Costas, E.; Hernandez, J.M. Shellfish consumption: A major risk factor for colorectal cancer. *Med. Hypotheses* **2008**, *70*, 409–412. [[CrossRef](#)] [[PubMed](#)]
79. Cordier, S.; Monfort, C.; Miossec, L.; Richardson, S.; Belin, C. Ecological Analysis of Digestive Cancer Mortality Related to Contamination by Diarrhetic Shellfish Poisoning Toxins along the Coasts of France. *Environ. Res.* **2000**, *84*, 145–150. [[CrossRef](#)] [[PubMed](#)]
80. López Rodas, V.; Maneiro, E.; Martínez, J.; Navarro, M.; Costas, E. Harmful algal blooms, red tides and human health: Diarrhetic shellfish poisoning and colorectal cancer. *Anales de la Real Academia Nacional de Farmacia* **2006**, *72*, 391–408.
81. Levin, E.D.; Pizarro, K.; Pang, W.G.; Harrison, J.; Ramsdell, J.S. Persisting behavioral consequences of prenatal domoic acid exposure in rats. *Neurotoxicol. Teratol.* **2005**, *27*, 719–725. [[CrossRef](#)] [[PubMed](#)]
82. Levin, E.D.; Pang, W.G.; Harrison, J.; Williams, P.; Petro, A.; Ramsdell, J.S. Persistent neurobehavioral effects of early postnatal domoic acid exposure in rats. *Neurotoxicol. Teratol.* **2006**, *28*, 673–680. [[CrossRef](#)] [[PubMed](#)]
83. Lefebvre, K.A.; Robertson, A. Domoic acid and human exposure risks: A review. *Toxicol.* **2010**, *56*, 218–230. [[CrossRef](#)] [[PubMed](#)]
84. Lefebvre, K.A.; Frame, E.R.; Gulland, F.; Hansen, J.D.; Kendrick, P.S.; Beyer, R.P.; Bammler, T.K.; Farin, F.M.; Hiolski, E.M.; Smith, D.R.; Marcinek, D.J. A Novel Antibody-Based Biomarker for Chronic Algal Toxin Exposure and Sub-Acute Neurotoxicity. *PLoS ONE* **2012**, *7*, e36213. [[CrossRef](#)] [[PubMed](#)]
85. Costa, L.G.; Giordano, G.; Faustman, E.M. Domoic acid as a developmental neurotoxin. *Neurotoxicology* **2010**, *31*, 409–423. [[CrossRef](#)] [[PubMed](#)]
86. Lefebvre, K.A.; Kendrick, P.S.; Ladiges, W.; Hiolski, E.M.; Ferriss, B.E.; Smith, D.R.; Marcinek, D.J. Chronic low-level exposure to the common seafood toxin domoic acid causes cognitive deficits in mice. *Harmful Algae* **2017**, *64*, 20–29. [[CrossRef](#)] [[PubMed](#)]
87. Grattan, L.M.; Boushey, C.; Tracy, K.; Trainer, V.; Roberts, S.M.; Schluterman, N.; Morris, J.G. The association between razor clam consumption and memory in the CoASTAL Cohort. *Harmful Algae* **2016**, *57*, 20–25. [[CrossRef](#)] [[PubMed](#)]

